Minimal-Energy Driving Strategy for High-Speed Electric Train With Hybrid System Model

Liang Li, *Member, IEEE*, Wei Dong, *Member, IEEE*, Yindong Ji, *Member, IEEE*, Zengke Zhang, and Lang Tong, *Fellow, IEEE*

***Abstract*—This paper studies a minimal-energy driving strategy for high-speed electric trains with a fixed travel time. A hybrid system model is proposed to describe the new characteristics of high-speed electric trains, including the extended speed range, energy efficiency, and regenerative braking. Based on this model, train driving is characterized by the gear sequence and the switching locations. An approximate gradient information is derived via the variational principle. To avoid a combinatorial explosion, the gear sequence is fixed by *a priori* knowledge. Then, a gradient-based exterior point method is proposed to calculate the optimal driving. In the case study, the minimal-energy driving with a fixed travel time for CRH-3 is investigated, and the result reveals some new understandings for high-speed electric train drive. Additionally, the tradeoff relationship between energy consumption and travel time is quantitatively studied, which is helpful in assigning an appropriate travel time for high-speed trains.**

***Index Terms*—Energy efficiency, high-speed electric tain, hybrid system model, marginal power, minimal-energy driving.**

I. Introduction

ELECTRIC trains, with their advantages of convenience and environmental performance, have been attracting increasing attention recently. Many countries in the world have begun to develop or expand their own electric train projects. However, this campaign is seriously impeded by the vast energy consumption of electric trains. Currently, there have been many techniques proposed to reduce the energy consumption of electric trains [1], such as adopting motorcoach patterns to make the train more compact and lighter, changing the outlook of locomotives to reduce the aerodynamic resistance, equipping the regenerative brake to feed back the kinetic energy, etc. On the other hand, a proper driving strategy can also reduce the energy consumption of electric trains. Many scholars and researchers have therefore been searching for the optimal driving strategy over the years.

The original research on optimal driving of electric trains was begun in the 1960s by Ichikawa [2], in which the optimization theory was primarily applied to train operation. The early mathematical model of trains took continuous control variables, such as acceleration and tractive effort, which facilitates investigation into optimal driving with the maximum principle (MP) [3]. In [4], train motion was formulated in the form of kinetic energy, and a parameterized optimal control effort was derived via the MP. The work in [5] took the relative tractive and braking forces as control variables and obtained a similar optimal control effort. The energy consumption of trains was expressed in the form of current and voltage in [6], and the MP was used to optimize the relative traction effort. Train driving can be also optimized by dynamic programming (DP) (see [7]). The nonlinear and constrained optimization problem in train operation can be handled by heuristic DP [8]. When discretizing the route line, discrete DP can be applied to optimize the tractive and brake efforts [9]. As the continuous control variable is not consistent with the actual train operation, these theoretical fruits did not received deserved attention from the industrial community.

Considering the operating mechanism of modern trains, Cheng and Howlett presented a model taking the discrete throttle as a control variable [10], in which each throttle corresponds to a traction power or a fuel supply rate. Based on this discrete model, the optimal driving strategy was respectively investigated on the level track with a speed limit [11] and on the nonzero slope track [12]. Furthermore, the necessary conditions for optimal control on the steep track were systematically studied in [13]. To simplify the throttle set, three throttles are usually considered in the given works, which correspond to the maximum traction, coasting, and maximum braking, respectively. It has been proven that any ideal strategy of continuous driving control can be approximated as closely as possible by these three throttles [11]. In fact, when considering the energy efficiency of throttles, this simplification may no longer be suitable. This will be illustrated later in this paper.

Based on previous works, the train driving between stations can be generally divided into four stages, i.e., traction, cruising, coasting, and braking. Therefore, the train driving can be characterized by the switching locations of stages. This turns out to be a nonlinear optimization problem. The metaheuristic methods were used to handle this kind of problem, e.g., genetic algorithm [14], tabu search, and ant colony optimization [15]. The simulated annealing algorithm in [16] was applied to search

Manuscript received March 11, 2012; revised August 12, 2012, January 8, 2013, and April 27, 2013; accepted May 21, 2013. Date of publication June 20, 2013; date of current version November 26, 2013. This work was supported in part by the Natural Science Foundation of China under Grants 61104019 and 61004070, by the National Key Technology Research and Development Program under Grant 2009BAG12A08, and by the Tsinghua University Initiative Scientific Research Program. The Associate Editor for this paper was A. Eskandarian.

L. Li, W. Dong, Y. Ji, and Z. Zhang are with the Department of Automation, Tsinghua University, and Tsinghua National Laboratory for Information Science and Technology, Beijing 100084, China (e-mail: liang-li07@mails.tsinghua.edu.cn; weidong@mail.tsinghua.edu.cn; jyd@mail.tsinghua.edu.cn; zzk@mail.tsinghua.edu.cn).

L. Tong is with the School of Electrical and Computer Engineering, Cornell University, Ithaca, NY 14853 USA (e-mail: ltong@ece.cornell.edu).

Color versions of one or more of the figures in this paper are available online at http://ieeexplore.ieee.org.

Digital Object Identifier 10.1109/TITS.2013.2265395

the cruising speed and the switching locations. With the help of improved computation capability, some simulation models were also presented to study the train's optimal driving [17]. A time-driven train performance simulation model was proposed in [18]. Based on this model, the energy consumption and trip time were studied with regard to the coasting position. The work in [19] developed an automatic-train-operation simulation model, which integrates a predictive fuzzy controller to regulate the speed profile.

However, modern electric trains, particularly high-speed trains, have greatly changed, and the past models can no longer describe the dynamics of high-speed trains. For example, because of an extended speed range, the dynamical property of high-speed trains is further divided into a "constant torque region" and a "constant power region." The discrete gears or settings, which control the train, should be attached with variable energy efficiencies. Additionally, the regenerative braking mechanism is introduced to save the energy, which feeds back the kinetic energy in the braking process. Therefore, a new mathematical model for modern electric trains is urgently needed to describe these new characteristics. In this paper, a hybrid system model is proposed to describe the dynamics of high-speed electric trains. Because of the nonlinearity and segmentation, the energy cost cannot be explicitly expressed by the switching locations, and a numerical solution is then presented to calculate the minimal-energy driving. On the other hand, it is found that the minimal energy consumption mainly depends on the preset travel time. Therefore, the conflicted relationship between energy consumption and travel time is also quantitatively investigated in this paper.

The remainder of this paper is organized as follows. In Section II, the new characteristics of high-speed electric trains are introduced. Section III proposes a hybrid system model and formulates the high-speed train's optimal driving problem. In Section IV-A, the gear sequence for optimal driving is studied. In Section IV-B, to calculate the optimal switching locations, the derivative of a cost function with respect to switching locations is investigated. In Section V, minimal-energy driving with a fixed running time is studied and a gradient-based algorithm is then presented, which is shown with a case study of CRH-3. Based on the former results, the conflicted relationship between energy consumption and the travel time is studied in Section VI. Finally, conclusions and recommendation for future works are given.

II. Characteristics of High-Speed Electric Trains

Modern trains are usually operated by discrete gears or throttles. Under each gear, a train is pulled with certain torque or power. Compared with traditional trains, the speed of modern trains has improved dramatically. In [20] and [21], the effort of a tractive motor is divided into a "constant torque region" and a "constant power region." In the constant torque region, a train runs within a low speed range and keeps a constant or linear tractive torque. In the constant power region, the train runs in a high speed range and takes a constant tractive or braking power.

For the low-speed train, the constant torque region is much narrower than the constant power region, and the train runs

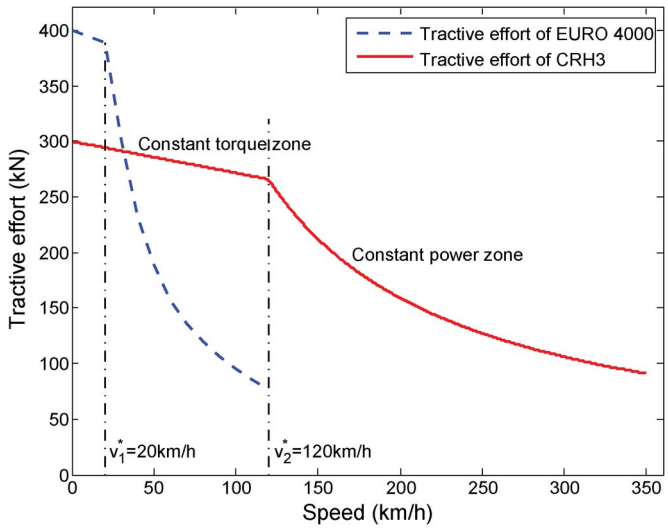

Fig. 1. Tractive effort curves of EURO 4000 and CRH-3.

in the constant power region at the most of the travel time. Therefore, in several early works, train models only considered the dynamics of the constant power region. With the speed increased, the constant torque region in the high-speed train can no longer be neglected. According to the definition given by the European Union, a high-speed train is "at a speed of at least 250 km/h on lines specially built for high speed" or "at a speed on the order of 200 km/h on existing lines" [22]. When considering the "constant torque region" and the "constant power region," both the tractive and brake characteristic curves turn out to be piecewise (see Fig. 1 for schematic curves of the tractive effort of the high-speed train CRH-3 and the traditional train EURO4000).

In this paper, it is assumed that the train has n tractive gears and m braking gears, and gear σ is donated as

$$\sigma \in \{-m, -m+1, \ldots, -1, 0, 1, \ldots, n-1, n\} \tag{1}$$

where $-m, -m+1, \ldots, -1$ are the braking gears, $1, \ldots, n-1, n$ are the tractive gears, and 0 refers to the coasting gear.

Based on the given analysis, the *constant torque model* for high-speed electric trains is formulated as

$$Mv\frac{dv}{dx} = F_\sigma - r(v) + g(x) \tag{2}$$

where M is the effective mass of a train and x is the position on the track. For the convenience of calculation, we take x as the independent variable here. $v(x)$ is the speed, which is a function of position x. F_σ is the constant tractive force in gear σ. $r(v)$ is the resistance force, and $g(x)$ is the component of gravitational force due to the track gradient at position x.

In addition, the *constant power model* for high-speed electric trains is

$$Mv\frac{dv}{dx} = \frac{P_\sigma}{v} - r(v) + g(x) \tag{3}$$

where P_σ is the power output in gear σ. Usually, the "constant power region" and the "constant torque region" are divided via a critical speed v^* (see v_1^* and v_2^* in Fig. 1).

To evaluate the energy consumption of the given driving scenario, there are usually two kinds of energy flows that need to be considered, i.e., the output energy and the feedback energy. The output energy can be further divided into the energy consumed in a propulsion system, the energy used in auxiliary machinery, and the energy losses in ventilation, air conditioning, lighting, and toilets. As the latter two terms are approximately constants and minor, the energy consumed in propulsion is merely considered in this paper, which accounts for the largest partition in output energy. The energy consumption in propulsion consists of the energy loss in aerodynamic resistance and the energy stored in a train, including potential energy and kinetic energy. When the train runs from position x_1 with speed v_1 to position x_2 with speed v_2, the energy consumed in propulsion can be expressed as

$$\Delta J = \int_{x_1}^{x_2} r(v)dx - \int_{x_1}^{x_2} g(x)dx + \frac{1}{2}M\left(v_2^2 - v_1^2\right). \quad (4)$$

The tractive motor of a train usually has an optimal operating region [23] and the energy efficiency changes with respect to different operation conditions [24]. In some literature, the efficiency of propulsion is taken as a constant coefficient, such as in [16] and [25]. The work in [26] investigated the factors affecting the energy efficiency of electric trains, which include the speed and the rates of acceleration and deceleration. Similarly, in [9] and [27], the energy efficiency of a train is expressed as a function of tractive force and speed. More tractive efforts and a higher speed always cause higher energy efficiency. In practice, the energy efficiency is an important factor considered when designing the driving strategy. There are some other factors affecting the energy efficiency of a propulsion system, such as load, acceleration, etc. In this paper, it is assumed that the energy efficiency only depends on the gear and speed. Therefore, the energy consumption in (4) should be modified as

$$\Delta J = \int_{x_1}^{x_2} F/\alpha(\sigma, v)dx. \quad (5)$$

Here, energy efficiency factor $\alpha(\sigma, v)$ is a function of gear σ and speed v, and takes a value between 0 and 1.

For the sake of energy saving, most electric trains are equipped with a regenerative brake [28]. When braking, the traction motor works in generator mode. The kinetic energy of a wheel is translated into electrical energy, which is then fed back into the electricity net or stored into the onboard battery. Similarly, the recovering efficiency of the regenerative brake also depends on brake effort and speed (for the detailed characteristics, see [6] and [29]). The feedback energy in the regenerative brake can be formulated as a function of gear and speed, i.e.,

$$\Delta J = \int_{x_1}^{x_2} \beta(\sigma, v)Fdx. \quad (6)$$

Here, recovering factor $\beta(\sigma, v)$ represents the percentage of feedback energy accounting for the total brake energy.

Remark 1: For the symbol's unification, the tractive force and the brake force are donated with the same symbol F in (4)–(6). In practice, F should be substituted with P_σ/v in the constant power region and with F_σ in the constant torque region. When in traction, F takes a positive value and the output power is also positive. When in regenerative braking, F takes a negative value and the energy in (6) is negative. In this case, the feedback energy should be comprehended as a negative output energy.

In summary, the four new characteristics considered for high-speed electric trains are: 1) the discrete-gear operating mechanism; 2) the dynamics of model autonomously switching between the "constant torque region" and the "constant power region"; 3) energy efficiency changing with respect to gears and speed; and 4) the regenerative brake attached with energy feedback.

III. Hybrid System Model and Problem Formulation

Here, a hybrid system model is introduced to cover the new characteristics of a high-speed electric train. The hybrid system is a dynamic system that exhibits both continuous and discrete dynamic behaviors [30], [31], in which the continuous dynamics are governed by a differential equation and the discrete dynamics are described by a logical graph. In [32] and [33], the dynamics of an electric train are modeled with a hybrid system, in which the dynamics of the train is simplified into a linear relationship and the control variables are the gear angle, the manifold pressure in continuous form, and the gear position in discrete form.

Typically, an extended automaton is proposed to represent the hybrid system, i.e., a hybrid automaton (HA) [34]. In this paper, a special HA is defined for a high-speed train. It is a six-tuple collection as follows:

$$H = \{D, C, f, I, S, G\} \quad (7)$$

where

- $D = \{\sigma\}$ is the set of operation modes. To distinguish the dynamics of the constant torque region and the constant power region, the gears in (1) are split as follows:

$$\sigma \in \{-m_{\mathrm{ct}}, -m_{\mathrm{cp}}, -(m-1)_{\mathrm{ct}}, -(m-1)_{\mathrm{cp}}, \ldots, -1_{\mathrm{ct}}, -1_{\mathrm{cp}}, 0, 1_{\mathrm{ct}}, 1_{\mathrm{cp}}, \ldots, (n-1)_{\mathrm{ct}}, (n-1)_{\mathrm{cp}}, n_{\mathrm{ct}}, n_{\mathrm{cp}}\}.$$

- $C = \{v, t\}$is the set of the continuous states, which consists of speed v and travel time t. Position x is taken as the independent variable here.
- $f : D \times C \to TC$ is the vector field, which governs the evolution of the continuous states. Referring to the differential equations (3) and (2), f should be a function vector $f = [f_1, f_2]^T$ formulated as

$$\begin{cases} \frac{dv}{dx} = f_1(\sigma, v) = \frac{1}{Mv}\left(F_\sigma - r(v) + g(x)\right) \\ \frac{dt}{dx} = f_2(\sigma, v) = \frac{1}{v} \end{cases} \quad (8)$$

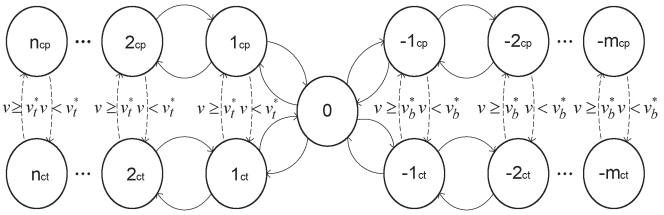

Fig. 2. HA for high-speed trains. The hard arrow is the controlled switching, and the dashed arrow is the autonomous switching. v_t^* and v_b^* are the critical speeds for tractive and braking efforts, respectively.

or

$$\begin{cases} \frac{dv}{dx} = f_1(\sigma, v) = \frac{1}{Mv}\left(\frac{P_\sigma}{v} - r(v) + g(x)\right) \\ \frac{dt}{dx} = f_2(\sigma, v) = \frac{1}{v}. \end{cases} \tag{9}$$

- $I \subseteq D \times C$ are the initial states of the train, including the continuous states and discrete modes.
- $S \subseteq D \times D$ is the allowable switch between operation modes. For high-speed train driving, the allowable switch consists of the controlled switches between gears and the autonomous switches between the constant torque region and the constant power region. In addition, the switch is assumed to be taking no time, but the Zeno behavior is not considered here.
- $G : S \to P(C)$ is the guard condition for switch S, which is usually a hyperplane on C. As there is autonomous switching between the constant torque mode and the constant power mode, the guard condition is the threshold of the critical speed v^*.

Typically, for an HA with a discontinuous switch, a reset term is introduced to update the state value after switching [35]. As the states of the train are continuous throughout the operation mode switching, the reset term is neglected here. (See Fig. 2 for an illustration of mode switching.)

As the autonomous switches between the constant torque region and the constant power region are mutually exclusive, the discrete state of the train is represented by gear σ only in the following content. For a certain driving, the gear sequence is donated as

$$\Sigma = \{\sigma_0, \sigma_1, \ldots, \sigma_i, \ldots, \sigma_N\} \tag{10}$$

where σ_i denotes the ith gear in the gear sequence and N is the number of switching gears. If the gear switching does not involve energy consumption, more gear switching results in better driving because it can arbitrarily control the speed curve with no cost. Obviously, this is not practical. In some literature, each gear switching is attached with a penalty cost. In this paper, the switching number is fixed with N. Moreover, the corresponding switching location sequence is

$$\Gamma = \{x_0, x_1, \ldots, x_i, \ldots, x_N\} \tag{11}$$

with $x_0 = 0$, $x_N = X$. X is the length of a journey. Gear σ_i is active in interval $[x_{i-1}, x_i]$. Therefore, a trajectory to the HA in (7) can be written as

$$\rho : (\sigma_0, v_{x_0}, t_{x_0}) \mapsto (\sigma_1, v_{x_1}, t_{x_1}) \mapsto \cdots (\sigma_N, v_{x_N}, t_{x_N}). \tag{12}$$

In practice, there are some constraints for train running. At first, the initial states of the train are fixed with

$$\sigma_0 = 0 \qquad v(x_0) = 0 \qquad t(x_0) = 0. \tag{13}$$

The running speed is limited by

$$v(x) \le V_{\max}(x) \tag{14}$$

where $V_{\max}(x)$ is the maximum permissible speed at position x.

Obviously, the train must stop at the destination station with a given travel time, i.e.,

$$v(x_N) = 0 \qquad t(x_N) = T \tag{15}$$

where T is the prespecified travel time.

Now, the following cost function is adopted to evaluate the energy consumption:

$$J = \sum_{i=1}^{N} \int_{x_{i-1}}^{x_i} L_{\sigma_i}(v, x)dx. \tag{16}$$

L_σ is a piecewise function, i.e.,

$$L_{\sigma_i} = \begin{cases} F_{\sigma_i}/\alpha(\sigma_i, v), & \sigma_i \ge 0; \quad v \le vt^* \\ P_{\sigma_i}/v/\alpha(\sigma_i, v), & \sigma_i \ge 0; \quad v \ge vt^* \\ \beta(\sigma_i, v)F_{\sigma_i}, & \sigma_i < 0; \quad v \le vb^* \\ \beta(\sigma_i, v)P_{\sigma_i}/v, & \sigma_i < 0; \quad v \ge vb^* \end{cases} \tag{17}$$

where $\alpha(\sigma_i, v)$ is the traction energy efficiency in (5) and $\beta(\sigma_i, v)$ is the regenerative energy efficiency in (6). vt^* is the critical speed of traction and vb^* is the critical speed of braking (see Fig. 2).

Finally, the minimal-energy driving problem for high-speed electric trains can be formally formulated as follows.

Problem 1: Find the switching gear sequence Σ and switching locations Γ to make the cost function J in (16) minimal, which is subjected to constraints in (7), (13)–(15).

IV. Solution

The given problem can be comprehended as the optimal control for the hybrid system with autonomous switching. The work in [36] presented a unified framework for optimal control of the hybrid system. In [37], the existence of optimal control for the hybrid system is analyzed with the MP. In this paper, as the length of the gear sequence is fixed and switching locations are in a closed interval, the existence of optimal driving is no doubt. In [38], a two-stage technology is proposed as follows: 1) Study the traditional optimal control problem with fixed discrete control sequence and find the switching instants and optimal control and 2) change the previous discrete control sequence and repeat step 1. Obviously, after searching all possible discrete sequences, the optimal driving strategy will be determined.

However, when adopting the given technology, the computation complexity will be intolerable. For driving, there are $(n + m + 1)^N$ possible gear sequences; therefore, the calculation amount is exponential with the length of the gear sequence.

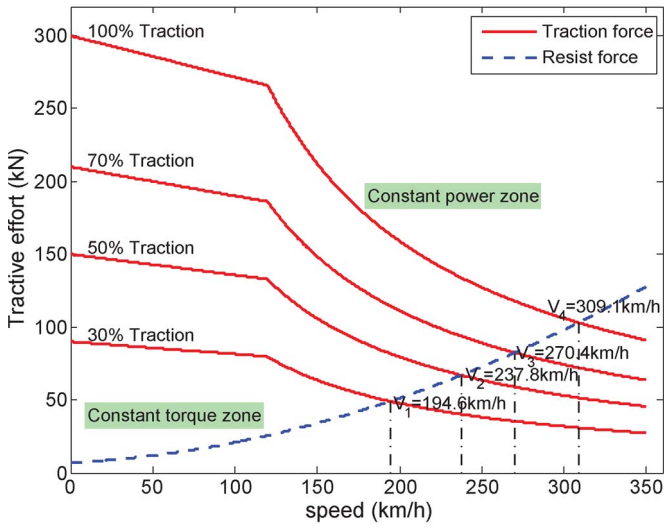

Fig. 3. Balance speeds of gears.

To avoid searching blindly for the space of the switching sequence, the gear sequence should be determined with *a priori* knowledge.

A. Gear Sequence

As aforementioned, the driving process can be divided into four stages, namely, traction, cruising, coasting, and braking. The following will analyze each stage and determine the gear sequence.

1) Cruising Stage: In the cruising stage, the train keeps a constant speed V_c. Usually, the constant speed is implemented via switching between two operation modes. For example, the cruising stage consists of maximum traction and coasting in [39]. For the high-speed train in this paper, constant speed V_c can be kept by switching between σ and $\sigma+1$ gears with

$$F_\sigma(V_c) \le r(V_c) + g(x) \le F_{\sigma+1}(V_c) \tag{18}$$

where $F_\sigma(V_c)$ is the traction effort under gear σ and speed V_c.

In fact, this strategy is only suitable for a freight train. For passenger trains, frequent switching between throttles σ and $\sigma+1$ makes the comfort poor. Therefore, it is sensible to choose a constant gear in the cruising stage. For each gear σ, there always exists balanced speed V_σ as follows:

$$\{V_\sigma \mid F_\sigma(V_\sigma) - r(V_\sigma) + g(x) = 0\}. \tag{19}$$

Therefore, the cruising speed is equal to balanced speed. (See Fig. 3 for balance speeds of the train with four gears.)

When the cruising stage dominates the trip time, cruising gear σ^* can be determined, whose balance speed is just greater than the average speed, i.e.,

$$\{\sigma^* \mid V_{\sigma^*-1} \le X/T \le V_{\sigma^*}\} \tag{20}$$

where trip time T and trip length X are given.

2) Traction Stage: In the traction stage, the train is accelerated to the cruising speed. Usually, there are two kinds of acceleration strategies. The first strategy switches traction gears from gear 1 to gear n with ascending order, which accelerates the train blandly and is good for the health of the train, but takes more time to reach the cruising speed. The other strategy accelerates the train from maximum traction gear n to gear 1. Of course, the advantage of this strategy is rapid, but the huge initial accelerator can destroy the train's health.

To investigate the two kinds of strategies, a mixed traction strategy is proposed here, which first adopts an ascending order of switching from gear 1 to gear n and then switches from gear n to cruising gear σ^* with descending order, i.e.,

$$\Sigma_t = \{1, 2, \ldots, n-1, n, n-1, \ldots, \sigma^*\}. \tag{21}$$

3) Braking Stage: There are two kinds of braking mechanisms in an electric train, i.e., regenerative braking and mechanical braking. The former is suitable for a high speed range, which translates the kinetic energy into electricity and then stores it. The latter is used for low speed without energy feedback. As a higher braking gear usually has higher efficiency of energy feedback, a descending-order braking strategy is taken here, i.e.,

$$\Sigma_b = \{-m, -m+1, \ldots, -1\}. \tag{22}$$

Once the gear sequence Σ is fixed, cost function J only depends on switching locations Γ, i.e.,

$$J(x_0, x_1, \ldots, x_N) = \sum_{i=1}^{N} \int_{x_{i-1}}^{x_i} L_{\sigma_i}(x, v)dx. \tag{23}$$

This is a nonlinear optimization problem. An exterior point method based on gradient information will be an option to calculate the optimal switching locations under a given gear sequence. Now, the gradient of the cost function with respect to locations is denoted as

$$\frac{dJ}{d\Gamma} = \left[\frac{\partial J}{\partial x_1}, \frac{\partial J}{\partial x_2}, \ldots, \frac{\partial J}{\partial x_{N-1}}\right]^T. \tag{24}$$

Here, the terminal conditions are fixed, i.e., $x_0 = 0$ and $x_N = X$.

If we can obtain the explicit expression of the cost function with respect to locations, the gradient $dJ/d\Gamma$ can be deduced analytically. However, from the differential equation of the constant power region in (3), only a hidden expression of speed and position can be obtained as

$$x - \int_0^{v(x)} \frac{\tau^2}{P_\sigma - a\tau - bv\tau - c\tau^3} d\tau + C_1 = 0 \tag{25}$$

where a, b, and c are fixed parameters, and C_1 depends on the initial values. Obviously, it is impossible to derive an explicit expression of the cost function from (23) and (25).

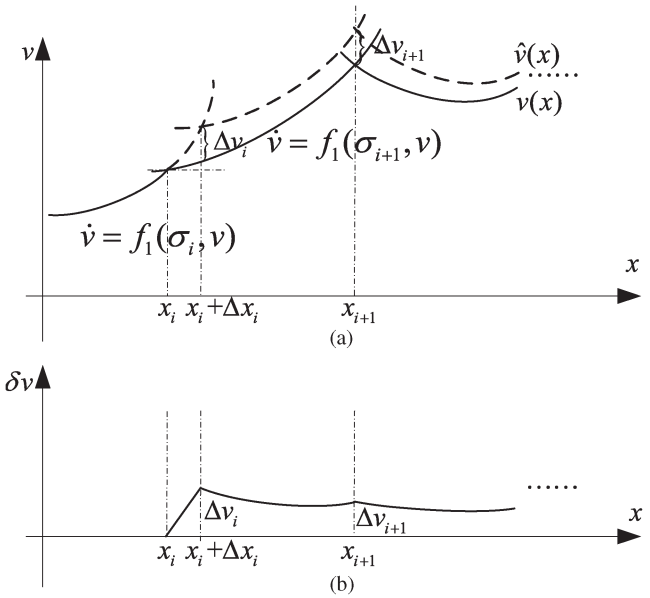

Fig. 4. Variational of the speed profile.

B. Derivation of the Switching Locations

Here, an approximate gradient information $dJ/d\Gamma$ will be calculated for the exterior point method. First, formulate the cost function on $[x_i, x_{i+1}]$ as

$$J_i = \int_{x_i}^{x_{i+1}} L_{\sigma_i}(x,\, v)dx. \tag{26}$$

Therefore, the total cost is

$$J = \sum_{i=0}^{N-1} J_i = \sum_{i=0}^{N-1} \int_{x_i}^{x_{i+1}} L_{\sigma_i}(x,\, v)dx. \tag{27}$$

According to (8) and (9), the speed evolution is reformulated as

$$\frac{dv}{dx} = f_1(\sigma_i, v, x), \quad x \in [x_i,\, x_{i+1}]. \tag{28}$$

In the following content, the variational method is adopted to calculate the partial derivative $\partial J/\partial x_i$. First, given a positive disturbance Δx_i to switching location x_i, this disturbance will cause a new speed profile, which is denoted as $\hat{v}$ [see Fig. 4(a)].

In $[x_i, x_i + \Delta x_i]$, write the Taylor expansion of the new speed profile as

$$\hat{v}(x) = v(x_i) + f_1(\sigma_i, v(x_i), x)(x - x_i) + o(x - x_i). \tag{29}$$

The corresponding variation to the speed profile is

$$\begin{aligned}\delta v(x) &= \hat{v}(x) - v(x)\\ &= \hat{v}(x) - (v(x_i) + f_1\,(\sigma_{i+1}, v(x_i), x)\\ &\qquad \times\,(x - x_i) + o(x - x_i))\\ &= [f_1\,(\sigma_i, v(x_i), x) - f_1(\sigma_{i+1}, v(x_i), x)]\\ &\quad \times\,(x - x_i) + o(x - x_i)\end{aligned} \tag{30}$$

and the speed change at $x_i + \Delta x$ is

$$\begin{aligned}\delta v(x_i + \Delta x) = [&f_1\,(\sigma_i, v(x_i), x)\\ &- f_1\,(\sigma_{i+1}, v(x_i), x)]\,\Delta x + o(x - x_i).\end{aligned} \tag{31}$$

In $[x_i + \Delta x_i, x_{i+1}]$, the differential equation for speed evolution is

$$\frac{d\hat{v}}{dx} = f_1(\sigma_{i+1}, \hat{v}, x). \tag{32}$$

In addition, the variation of speed can be expressed in a differential equation as

$$\begin{aligned}\frac{d(\delta v)}{dx} &= f_1(\sigma_{i+1}, \hat{v}, x) - f_1(\sigma_{i+1}, v, x)\\ &= \frac{\partial f_1(\sigma_{i+1}, v, x)}{\partial v}(\hat{v} - v) + o(\hat{v} - v)\\ &\simeq \frac{\partial f_1(\sigma_{i+1}, v, x)}{\partial v}\delta v.\end{aligned} \tag{33}$$

Let us introduce a state transition function $T_k(x_1, x_2)$ for differential equation $(d(\delta v)/dx) = (\partial f_1(\sigma_{k+1}, v, x)/\partial v)\delta v$, $k = i, \ldots, N-1$ as follows:

$$\delta v(x_2) = \delta v(x_1)T_k(x_1, x_2), \qquad x_k \le x_1 \le x_2 \le x_{k+1}. \tag{34}$$

The speed variable in (33) can be formulated as

$$\delta v(x) = \delta v(x_i + \Delta x_i)T_i(x_i + \Delta x_i, x), \quad x \in [x_i + \Delta x_i, x_{i+1}] \tag{35}$$

and for $k = i+1, \ldots, N-1$, we have

$$\delta v(x) = \delta v(x_k)T_k(x_k, x), \quad x \in [x_k, x_{k+1}]. \tag{36}$$

The cost function can be rewritten as

$$\begin{aligned}\hat{J} &= \sum_{j=0}^{N-1} \hat{J}_j\\ &= \sum_{j=0,\, j\neq i}^{N-1} \int_{x_j}^{x_{j+1}} L_{\sigma_j}(x, \hat{v})dx + \int_{x_i}^{x_i + \Delta x_i} L_{\sigma_i}(x, \hat{v})dx\\ &\quad + \int_{x_i + \Delta x_i}^{x_{i+1}} L_{\sigma_{i+1}}(x, \hat{v})dx.\end{aligned} \tag{37}$$

Then, we expand it at the original speed profile $v(x)$ with the Taylor series and obtain the disturbance of cost in (38). According to (31) and (36), when we take $\Delta x_i \to 0$, the disturbance of cost in (38) can be expressed as (39), as shown in

$$\begin{aligned}\Delta J &= \hat{J} - J\\ &= \int_{x_i}^{x_i + \Delta x_i} \left(\frac{\partial L_{\sigma_i}}{\partial v} - 2\frac{\partial L_{\sigma_{i+1}}}{\partial v}\right)\delta v dx\\ &\quad + \sum_{j=i}^{N-1} \left\{ \int_{x_j}^{x_{j+1}} \frac{\partial L_{\sigma_{j+1}}}{\partial v}\delta v dx \right\} + o(\delta v)\end{aligned} \tag{38}$$

$$= \left(\frac{\partial L_{\sigma_i}}{\partial v} - 2\frac{\partial L_{\sigma_{i+1}}}{\partial v}\right)\delta v \Delta x_i + \sum_{j=i}^{N-1}\left\{\int_{x_j}^{x_{j+1}} \frac{\partial L_{\sigma_{j+1}}}{\partial v}\delta v dx\right\} + o(\Delta x_i) \qquad (\Delta x_i \to 0)$$

$$= \left(f_1\left(\sigma_i, v(x_i), x\right) - f_1\left(\sigma_{i+1}, v(x_i), x\right)\right) \times \Delta x \left(\sum_{j=i}^{N-1}\int_{x_j}^{x_{j+1}} \frac{\partial L_{\sigma_{j+1}}}{\partial v}\left(\Pi_{k=i}^{j-1} T_k(x_k, x_{k+1})\right) \times T_j(x_j, x)dx\right) + o(\Delta x_i) \qquad (39)$$

$$\simeq \left(f_1\left(\sigma_i, v(x_i), x\right) - f_1\left(\sigma_{i+1}, v(x_i), x\right)\right) \times \Delta x \int_{x_i}^{x_{i+1}} \left(\frac{\partial L_{\sigma_{i+1}}}{\partial v} T_i(x_i, x)\right) dx + o(\Delta x_i). \qquad (40)$$

In practice, the disturbance of speed in (36) always decays dramatically. An approximate expression for the disturbance of speed is

$$\delta v(x) = \begin{cases} \delta v(x_i + \Delta x_i) T_i(x_i, x), & x \in [x_i, x_{i+1}] \\ 0, & x \in [x_{i+1}, x_N] \end{cases} \qquad (41)$$

and the disturbance of cost in (39) can be further simplified as in (40).

Finally, the derivative of the cost function with respect to the switching locations x_i can be approximately formulated as

$$\frac{\partial J}{\partial x_i} = \left[f_1\left(\sigma_i, v(x_i), x\right) - f_1\left(\sigma_{i+1}, v(x_i), x\right)\right] \times \int_{x_i}^{x_{i+1}} \frac{\partial L_{\sigma_{i+1}}}{\partial v} T_i(x_i, x)dx \qquad (42)$$

where $i \neq 0, N$ as the initial and terminal instants are fixed. In addition, the second-order gradient information $\partial^2 J/\partial^2 x_i$ can also be calculated based on the given result (see [40]).

V. Optimal Driving With Fixed Travel Time

For optimal driving, there still are three constraints to be satisfied, namely, initial constraints in (13), speed limitation in (14), and the terminal condition in (15). Given trip time T, we extend the cost function in (16) as

$$J_E = \sum_{i=1}^{N}\int_{x_{i-1}}^{x_i} L_\sigma(v, x)dx + \gamma\left(\sum_{i=1}^{N}\int_{x_{i-1}}^{x_i}\frac{1}{v}dx - T\right)^2. \qquad (43)$$

Here, γ is a penalty factor that can force the speed profile to satisfy the trip time constraint.

As the boundary conditions are difficult to satisfy in unidirectional calculation, a forward integration is adopted to calculate the speed profile in traction and cruising stages, and a backward integration is adopted to calculate the speed profile in the braking and coasting stages. Therefore, the boundary conditions are held through picking appropriate initial values

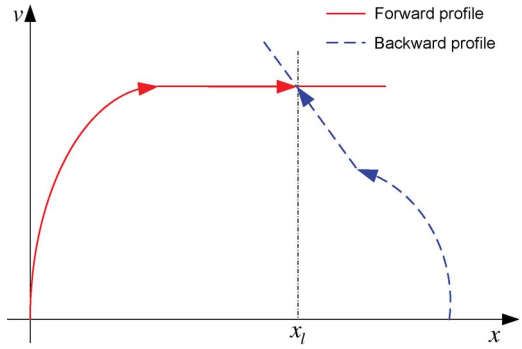

Fig. 5. Forward profile and backward profile.

in both integrations, and the two profiles meet at a switching location x_l (see Fig. 5).

The extended gradient in the forward profile is

$$\frac{\partial J_E}{\partial x_i} = \left(f_1(\sigma_i, x_i) - f_1(\sigma_{i+1}, x_i)\right)\left[\int_{x_i}^{x_{i+1}} \frac{\partial L_{\sigma_i+1}}{\partial v} T_i(x_i, x)dx - 2\gamma\left(\sum_{k=1}^{l}\int_{x_{i-1}}^{x_i}\frac{1}{v}dx - T\right)\int_{x_i}^{x_{i+1}}\frac{1}{v^2}T_i(x_i, x)dx\right] \qquad (44)$$

with $0 < x_i < x_l$.

The extended gradient in the backward profile is

$$\frac{\partial J_E}{\partial x_j} = \left(f_1(\sigma_{j+1}, x_j) - f_1(\sigma_j, x_j)\right)\left[\int_{x_j}^{x_{j-1}} \frac{\partial L_{\sigma_j-1}}{\partial v} T_j(x_j, x)dx - 2\gamma\left(\sum_{k=N}^{l}\int_{x_i}^{x_{i-1}}\frac{1}{v}dx - T\right)\int_{x_j}^{x_{j-1}}\frac{1}{v^2}T_j(x_j, x)dx\right] \qquad (45)$$

with $x_N > x_j > x_l$. Note that x_l is the meeting location, and the gradient $\partial J_E/\partial x_l$ is not defined here. Additionally, when the speed profile violates the limitation in (14), it only forces the profile below the permission speed.

In this paper, a gradient-based exterior point method is proposed to optimize the driving strategy. The exterior point method is a kind of a penalty method, and its initial value is not necessary to be feasible. As it is difficult to pick an initial value to satisfy the trip time constraint, the exterior point method is reasonable here. The gradient information is used to guide the evolution of solution (see [41] for the proof of its convergence). The detailed procedure is given in Algorithm 1.

Algorithm 1 a gradient-based exterior point method.

Require:
track length X, travel time T
Ensure:
gear sequence Σ, switching locations Γ, energy cost J
1) determine the cruising gear σ^* with

$$v_{\sigma^*-1} \leq X/T \leq v_{\sigma^*}$$

2) fix the initial gear sequence

$$\Sigma = \{1, \ldots, n, n-1, \ldots, \sigma^*, -m, -m+1, \ldots, -1\}$$

3) initialize the switching locations and iterative label k

$$\Gamma_0 = [x_1, x_2, \ldots, x_{N-1}]^T, k = 0$$

4) solve speed profiles using a fourth-order Runge–Kutta method
   - forward profile in $[x_0, x_l]$ with $v(x_0) = 0$
   - $v_i(x) = \text{ode45}(f_{\sigma_i}, [x_{i-1}, x_i], v(x_{i-1}))$, $i = 1, \ldots, l$
   - backward profile in $[x_l, x_N]$ with $v(x_N) = 0$
   - $v_j(x) = \text{ode45}(f_{\sigma_j}, [x_j, x_{j-1}], v(x_j))$, $j = N, \ldots, l+1$

5) calculate the gradient information with (44), (45)

$$\frac{dJ_E}{d\Gamma_k} = \left[\frac{\partial J_E}{\partial x_1}, \frac{\partial J_E}{\partial x_2}, \ldots, \frac{\partial J_E}{\partial x_{N-1}}\right]^T$$

6) update the switching locations

$$\Gamma_{k+1} = \Gamma_k + h\left(\frac{dJ_E}{d\Gamma_k}\right)^T$$

7) get the cost function J_{k+1} with (43)
8) evaluate the terminal condition

$$\left|\frac{J_{k+1} - J_k}{J_{k+1}}\right| \leq \delta$$

9) **repeat**
10) steps 4, 5, 6, 7, and 8
11) **until** the terminal condition is satisfied
12) **return** Σ, Γ, J

Remark 2: As the magnitude values of the energy term and the time term in the cost function are dramatically mismatched, the gradient-based algorithm proposed here may oscillate seriously. First, a large initial penalty factor γ can quickly force the speed profile to satisfy the journey time constraint. Then, the energy consumption is minimized with an increased penalty factor. Therefore, the penalty factor in this algorithm should not been tuned in a strictly increasing order.

Remark 3: In this algorithm, the gear sequence is fixed with *a priori* knowledge of train driving. In fact, it can also calculate the optimal switching locations for an arbitrary feasible gear sequence.

A. Case Study

Here, the optimal driving for the high-speed electric train CRH-3 is studied, which is a version of the Siemens Velaro high-speed train used in China. A track interval is chosen on the Beijing–Tianjin Intercity Railway with length $L = 72$ km and the travel time is fixed as $T = 1200$ s. The main parameters of CRH-3 are listed in Table I. The maximum tractive and braking forces are

TABLE I
PARAMETERS OF CRH-3

Mass(t)	408	Motor type	MT205
Frontal area(m^2)	9	Out power(kW)	300×16
The number of cars	8	Voltage rating(V)	2000
The numbers of axles	32	Current rating(A)	106

TABLE II
PARAMETERS OF GEARS

index (σ)	effort (F_σ)	balance speed (V_σ)	efficiency (α, β)[a]
4	F_{mt}	85.86m/s	0.7
3	$0.7F_{mt}$	75.11m/s	0.9[b]
2	$0.5F_{mt}$	66.06m/s	0.75
1	$0.3F_{mt}$	54.05m/s	0.6
0	0	None[c]	0
-1	$0.3F_{mb}$	None[d]	0
-2	$0.5F_{mb}$	None	0.6
-3	$0.7F_{mb}$	None	0.75
-4	F_{mb}	None	0.9

[a] generally, efficiency coefficient α, β is considered as a function of speed v and gear σ. Because of limit of computation ability, it's assigned a constant efficiency for each gear in this case.
[b] this is the most efficient tractive gear, which works in the optimal operating region [23].
[c,d] there is no balance speed for coasting and braking.

$$F_{\text{mt}} = \begin{cases} 300 - 0.284v & 0 \leq v \leq 119.7 \text{ km/h} \\ 266 \times 119.7/v & 119.7 \leq v \leq 300 \text{ km/h} \end{cases}_{(kN)}$$

$$F_{\text{mb}} = \begin{cases} -300 + 0.281v & 0 \leq v \leq 106.7 \text{ km/h} \\ -270 \times 106.7/v & 106.7 \leq v \leq 300 \text{ km/h} \end{cases}_{(kN).}$$

The resistant and frictional forces are summarized in the term $r(v)$. The frictional force is mainly an adhesive force caused by the contact between the wheel and the track surface, and the resistance consists of bearing or resistance, flange resistance, and aerodynamic resistance. Here, we adopt the experiential expression in [16] as

$$r(v) = 6.4M + 130q + 0.14Mv + [0.046 + 0.0065(p-1)]\,Av^2 \tag{46}$$

where M is the actual mass in tons, q is the number of axles, p is the number of cars in the train, and A is the frontal area in square meters. Substituting the parameters of CRH-3 in Table I into (46), the sum of the resistant and frictional forces can be expressed as

$$r(v) = 6774.4 + 57.19v + 0.8235v^2 \tag{47}$$

where v is the speed in kilometers per hour and $r(v)$ is the resistance in newtons.

In practice, the gear number of a high-speed train is more than 8 or even 13. For simplification of computation, it is assumed that the high-speed train works in four tractive gears and four braking gears. The properties of each gear are shown in Table II. F_{mt} is the maximum tractive force and F_{mb} is

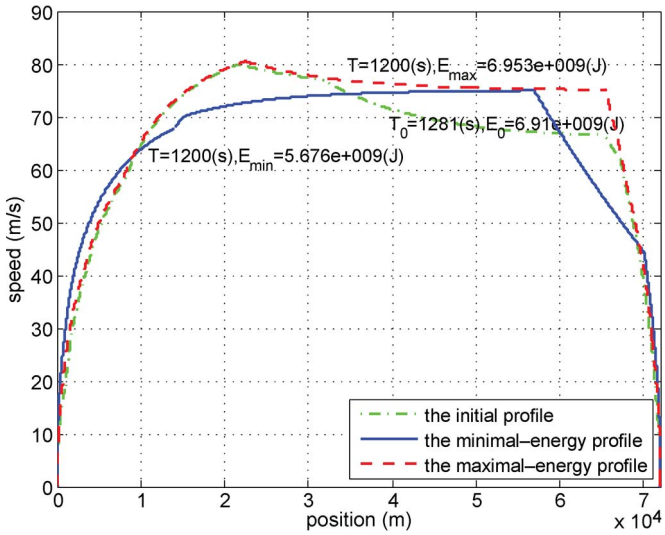

Fig. 6. Minimal-energy and maximal-energy driving profiles with travel time $T = 1200$ s.

the maximum braking force. Brake gear -1 is taken as mechanical braking without energy feedback; therefore, its energy efficiency is zero.

As the average speed is $\bar{v} = 72000/1200 = 60$ m/s, the cruising gear is first fixed as 2 by $v_1 < \bar{v} < v_2$. The initial gear sequence is

$$\Sigma_0 = \{1, 2, 3, 4, 3, 2, 0, -4, -3, -2, -1\}$$

and we assign an arbitrary switching locations as

$$\Gamma_0 = \{1000, 3570, 8050, 21800, 31800, x_l, 67200, 68200, 70400, 71600\}_m.$$

Here, the meeting location of forward and backward profiles is $x_l = 65\,283$ m. With the given initial speed profile and travel time T, apply the proposed algorithm to calculate the minimal-energy driving as

$$\Sigma_{\min} = \{3, 4, 3, 0, -4, -3\}$$
$$\Gamma_{\min} = \{14013, 15151, 56921, 70049, 70429\}_m.$$

The minimal energy consumption is $E_{\min} = 5.676 \times 10^9$ J.

On the other hand, the worst driving is also interesting with a given travel time and gear sequence. Using the negative gradient information in (44) and (45) calculates the maximal-energy driving under the same travel time. The switching locations and gear sequence are listed as

$$\Sigma_{\max} = \{1, 2, 3, 4, 3, -4, -3, -2, -1\}$$
$$\Gamma_{\max} = \{223, 3296, 7877, 22582, 65401, 68121, 70963, 71997\}_m.$$

The maximal energy consumption is $E_{\max} = 6.953 \times 10^9$ J. The speed profiles and gear sequences for the two drives are shown in Figs. 6 and 7. It is found that some unnecessary gears are discarded in tractive and braking stages, and the coasting range is extended in minimal-energy driving, whereas the opponent phenomenon appears in the maximal-energy driving.

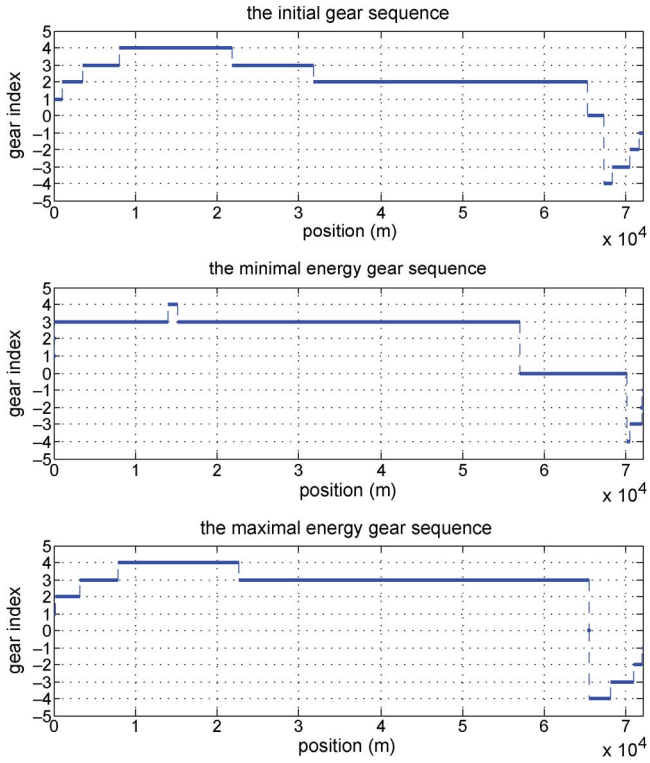

Fig. 7. Minimal-energy and maximal-energy driving gear sequence.

B. Some New Understanding

From the different driving strategies, this paper obtains the following interesting comprehension for high-speed electric train driving. First, with a given travel time, the best and worst driving strategies may have a huge difference on energy consumption. For example, in the case study earlier, by fixing the travel time $T = 1200$ s, the best driving saves 18.37% energy compared with the worst driving. Second, in the tractive stage, the gears with the highest efficiency will be considered first. The gear with the maximal effort is introduced to satisfy the travel time constraint, e.g., the fourth tractive gear. Third, the highest efficiency braking gear is not necessary in the braking stage, and a lower efficiency gear may be the better compromise between the energy feedback and the travel time constraint. Finally, to stop the train, the coasting gear is always the better choice than any braking gear. Intuitively, the regenerative braking should be the first choice in the braking stage. However, in the case study given, the coasting stage is extended in the minimal-energy driving, whereas it is discarded in the maximal-energy driving. In fact, as long as the regenerative braking cannot completely feed back the kinetic energy, the coasting is the most efficient way to stop the train.

VI. Relationship Between Energy Consumption and Travel Time

Earlier, the energy consumption of driving is minimized under the constraint of a fixed travel time. What will happen if we give up the fixed travel time? Intuitionally, reducing the travel time causes the energy consumption in driving to increase, and extending the travel time provides a possibility to consume less

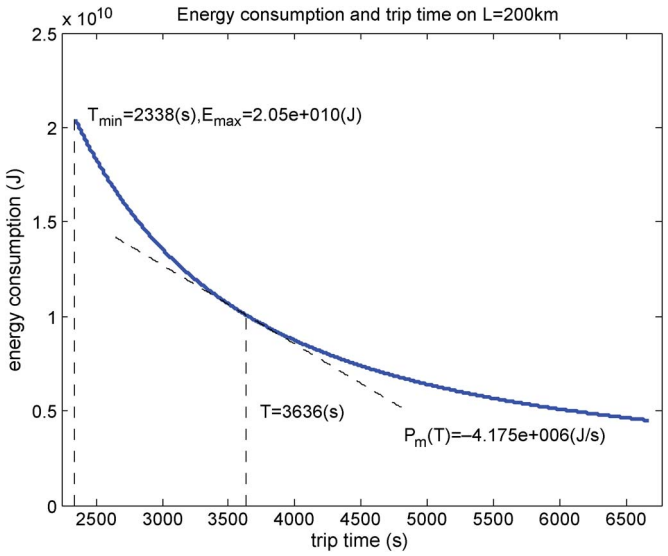

Fig. 8. Relationship of journey time T and energy consumption E.

energy in driving. The work in [42] first discusses the conflicted relationship between energy consumption and travel time, and then introduces the Pareto efficiency into train driving. In [43], Pareto curves for high-speed train driving are investigated via computer simulation. In addition, the tradeoff relationship in train driving is investigated in [44]. Here, we investigate the quantitative relationship between energy consumption and travel time.

In general, it is difficult to get an analytical expression between energy consumption and travel time on a given track. Among the four stages of the driving process, the cruising stage usually consumes most of the energy on a long track, whereas the energy consumption of the other three stages are relatively constant. When denoting the length of the cruising stage as X_c and its running time as T_c, the average speed in cruising is

$$V_c = \frac{X_c}{T_c}. \tag{48}$$

In the cruising stage, the energy is mainly used to resist force $r(v)$. Therefore, the energy consumption in the cruising stage can be expressed as

$$E_c = r(V_c)X_c. \tag{49}$$

When the track line is long enough, it is reasonable to use (48) and (49) to approximately express the conflicted relationship between energy consumption and travel time on the whole line, i.e.,

$$E = r\left(\frac{X}{T}\right)X. \tag{50}$$

For example, taking the $r(v)$ in (47), the energy consumption of CRH-3 can be expressed as (see Fig. 8)

$$E = 6774.4X + 205.88\frac{X^2}{T} + 10.67\frac{X^3}{T^2}. \tag{51}$$

It turns out that energy consumption is a hyperbolic function of travel time, which means that the energy cost increases for each reduced unit of travel time. It is very useful to introduce the concept of marginal power to measure the energy cost of travel time cutting, which is defined as the energy consumption for every second cut in travel time, i.e.,

$$P_m = \frac{\Delta E}{\Delta T}. \tag{52}$$

Based on (51), the marginal power for CRH-3 can be approximately formulated as

$$P_m(T) = -205.88\frac{X^2}{T^2} - 21.34\frac{X^3}{T^3}. \tag{53}$$

This is similar to the marginal benefit in economics. From the passengers' perspective, shortening the travel time is always a good thing. However, unwisely reducing the travel time is unreasonable in some situation because the energy consumption may sharply increase with respect to each unit of travel time cut. On the other hand, a train operator always intends to extend travel time to save energy. With the help of marginal power, it is possible to evaluate the energy cost of changing the recent travel time and to find a tradeoff scheme.

VII. Conclusion

In this paper, the optimal driving for high-speed electric trains has been investigated. A hybrid system model for trains is presented to satisfy the new properties of high-speed electric trains, which includes the extended speed range, the operated gears with energy efficiencies, and regenerative braking. With the gear sequence fixed by *a priori* knowledge, the optimal driving for the high-speed electric train turns out to be a nonlinear optimization problem. Because there is no explicit expression of energy cost with respect to switch locations, an exterior point method is proposed to calculate the minimal- and maximal-energy driving strategies. In the minimal-energy driving, the most efficient gear dominates the tractive and cruising stages, whereas the highest speed gear is adopted to satisfy the travel time constraint. Contrary to the intuitive understanding, coasting is more efficient than regenerative braking in the case study. At last, the concept of marginal power is introduced to evaluate the efficiency of changing the travel time. A reasonable travel time is definitely the best way to save energy in high-speed train driving. There are still some future works about high-speed train driving. For example, this paper just treats the energy efficiency as the constant values because of the bottleneck of computation amount. An efficient and powerful optimization algorithm is urgently needed in the future.

References

[1] S. Kobayashi, S. Plotkin, and S. K. Ribeiro, "Energy efficiency technologies for road vehicles," *Energy Efficiency*, vol. 2, no. 1, pp. 125–137, May 2009.

[2] I. Kunihiko, "Application of optimization theory for bounded state variable problems to the operation of train," *Bull. Jpn. Soc. Mech. Eng.*, vol. 11, no. 47, pp. 857–865, Nov. 1968.

[3] I. A. Asnis, A. V. Dmitruk, and N. P. Osmolovskii, "Solution of the problem of the energetically optimal-control of the motion of a train by

the maximum principle," *USSR Comput. Math. Math. Phys.*, vol. 25, no. 6, pp. 37–44, 1985.
[4] E. Khmelnitsky, "On an optimal control problem of train operation," *IEEE Trans. Autom. Control*, vol. 45, no. 7, pp. 1257–1266, Jul. 2000.
[5] R. Liu and I. M. Golovitcher, "Energy-efficient operation of rail vehicles," *Transp. Res. Part A, Policy Pract.*, vol. 37, no. 10, pp. 917–932, Dec. 2003.
[6] M. Miyatake and H. Ko, "Optimization of train speed profle for minimum energy consumption," *IEEJ Trans. Elect. Electron. Eng.*, vol. 5, no. 3, pp. 263–269, May 2010.
[7] H. Ko, T. Koseki, and M. Miyatake, "Application of dynamic programming to the optimization of the running profile of a train," in *Computers in Railway SIX*. Southampton: WIT Press, 2004, pp. 103–112.
[8] W. S. Lin and J. W. Sheu, "Automatic train regulation for metro lines using dual heuristic dynamic programming," *Proc. Inst. Mech. Eng. Part F, J. Rail Rapid Transit*, vol. 224, no. F1, pp. 15–23, Jan. 2010.
[9] R. Franke, P. Terwiesch, and M. Meyer, "An algorithm for the optimal control of the driving of trains," in *Proc. 39th IEEE Conf. Decision Control*, 2000, vol. 3, pp. 2123–2128.
[10] J. X. Cheng and P. Howlett, "Application of critical velocities to the minimization of fuel consumption in the control of trains," *Automatica*, vol. 28, no. 1, pp. 165–169, Jan. 1992.
[11] P. G. Howlett, I. P. Milroy, and P. J. Pudney, "Energy-efficient train control," *Control Eng. Pract.*, vol. 2, no. 2, pp. 193–200, Apr. 1994.
[12] P. G. Howlett, P. J. Pudney, and X. Vu, "Local energy minimization in optimal train control," *Automatica*, vol. 45, no. 11, pp. 2692–2698, Nov. 2009.
[13] X. Vu, "Analysis of necessary conditions for the optimal control of a train," Ph.D. dissertation, Univ. South Australia, Adelaide, SA, Australia, 2006.
[14] G. Acampora, C. Landi, M. Luiso, and N. Pasquino, "Optimization of energy consumption in a railway traction system," in *Proc. SPEEDAM*, 2006, pp. 1121–1126.
[15] B.-R. Ke, C.-L. Lin, and C.-W. Lai, "Optimization of train-speed trajectory and control for mass rapid transit systems," *Control Eng. Pract.*, vol. 19, no. 7, pp. 675–687, Jul. 2011.
[16] K. Kim and S. I.-J. Chien, "Optimal train operation for minimum energy consumption considering track alignment, speed limit, and schedule adherence," *J. Transp. Eng.*, vol. 137, no. 9, pp. 665–674, Sep. 2011.
[17] C. J. Goodman, L. K. Siu, and T. K. Ho, "A review of simulation models for railway systems," in *Proc. Int. Conf. Dev. Mass Transit Syst.*, London, U.K., 1998, pp. 80–85.
[18] K. Kim and S. I.-J. Chien, "Simulation-based analysis of train controls under various track alignments," *J. Transp. Eng.*, vol. 136, no. 11, pp. 937–948, Nov. 2010.
[19] S. Yasunobu and S. Miyamoto, "Automatic train operation system by predictive fuzzy control," in *Industrial Applications of Fuzzy control*. Amsterdam, The Netherlands: Elsevier, 1985, pp. 1–18.
[20] S. Lu, S. Hillmansen, and C. Roberts, "A power-management strategy for multiple-unit railroad vehicles," *IEEE Trans. Veh. Technol.*, vol. 60, no. 2, pp. 406–420, Feb. 2011.
[21] F. Schmid and C. J. Goodman, "Electric railway systems in common use," in *Proc. 5th IET Professional Dev. Course REIS*, 2011, pp. 1–15.
[22] General definitions of highspeed 2009.
[23] K. T. Chau and Y. S. Wong, "Overview of power management in hybrid electric vehicles," *Energy Convers. Manage.*, vol. 43, no. 15, pp. 1953–1968, Oct. 2002.
[24] J. Faiz and M. B. B. Sharifian, "Optimal design of an induction motor for an electric vehicle," *Eur. Trans. Elect. Power*, vol. 16, no. 1, pp. 15–33, Jan. 2006.
[25] W. W. Hay, *Railroad Engineering*, 2nd ed. New York, NY, USA: Wiley, 1982.
[26] N. Iwai, "Analysis on fuel economy and advanced systems of hybrid vehicles," *JSAE Rev.*, vol. 20, no. 1, pp. 3–11, Jan. 1999.
[27] J. C. Jong and E. F. Chang, "Models for estimating energy consumption of electric train," *J. Eastern Asia Soc. Transp. Stud.*, vol. 6, pp. 278–291, 2005.
[28] M. Miyatake and H. Ko, "Numerical analyses of minimum energy operation of multiple trains under dc power feeding circuit," in *Proc. Eur. Conf. Power Electron. Appl.*, 2007, pp. 1–10.
[29] Z. Rahman, M. Ehsani, and K. L. Butler, "An investigation of electric motor drive characteristics for EV and HEV propulsion systems," presented at the Future Transportation Technol. Conf. Expo., Costa Mesa, CA, USA, 2000, Paper 2000-01-3062.
[30] A. Gollu and P. Varaiya, "Hybrid dynamical systems," in *Proc. Conf. Decision Control*, Dec. 13–15, 1989, vol. 3, pp. 2708–2712.
[31] R. Goebel, R. G. Sanfelice, and A. R. Teel, "Hybrid dynamical systems," *IEEE Control Syst.*, vol. 29, no. 2, pp. 28–93, Apr. 2009.
[32] L. Y. Wang, A. Beydoun, J. Cook, J. Sun, and I. Kolmanovsky, "Optimal hybrid control with applications to automotive powertrain systems," in *Proc. Control Using Logic-Based Switching*, vol. 222, *Lecture Notes Control Information Sciences*, 1997, pp. 190–200.
[33] A. Beydoun, L. Y. Wang, J. Sun, and S. Sivashankar, "Hybrid control of automotive powertrain system: A case study," in *Proc. 1st Int. Workshop HSCC*, London, U.K., 1998, pp. 33–48.
[34] T. A. Henzinger, "The theory of hybrid automata," in *Verification of Digital and Hybrid System*. Berlin, Germany: Springer-Verlag, 2000, pp. 265–292.
[35] J. Lygeros, K. H. Johansson, S. N. Simic, J. Zhang, and S. S. Sastry, "Dynamical properties of hybrid automata," *IEEE Trans. Autom. Control*, vol. 48, no. 1, pp. 2–17, Jan. 2003.
[36] M. S. Branicky, V. S. Borkar, and S. K. Mitter, "A unified framework for hybrid control: Model and optimal control theory," *IEEE Trans. Autom. Control*, vol. 43, no. 1, pp. 31–45, Jan. 1998.
[37] H. J. Sussmann, "A maximum principle for hybrid optimal control problems," in *Proc. 38th IEEE Conf. Decision Control*, 1999, vol. 1, pp. 425–430.
[38] X. Xu and P. J. Antsaklis, "Optimal control of switched systems based on parameterization of the switching instants," *IEEE Trans. Autom. Control*, vol. 49, no. 1, pp. 2–16, Jan. 2004.
[39] P. Howlett, "Optimal strategies for the control of a train," *Automatica*, vol. 32, no. 4, pp. 519–532, Apr. 1996.
[40] X. Xuping and P. J. Antsaklis, "Optimal control of switched autonomous systems," in *Proc. IEEE CDC*, Dec. 10–13, 2002, vol. 4, pp. 4401–4406.
[41] J. F. Andrus, "An exterior point method for the convex-programming problem," *J. Optim. Theory Appl.*, vol. 72, no. 1, pp. 37–63, Jan. 1992.
[42] S. Talukdar and R. Koo, "Multi-objective trajectory optimization for electric trains," *IEEE Trans. Autom. Control*, vol. AC-24, no. 6, pp. 888–893, Dec. 1979.
[43] C. Sicre, P. Cucala, A. Fernandez, J. A. Jimenez, I. Ribera, and A. Serrano, "A method to optimise train energy consumption combining manual energy efficient driving and scheduling," in *Computers in Railways XII: Computer System Design and Operation in Railways and Other Transit Systems*. Southampton, U.K.: WIT Press, 2010, pp. 549–560.
[44] H.-S. Hwang, "Control strategy for optimal compromise between trip time and energy consumption in a high-speed railway," *IEEE Trans. Syst., Man, Cybern. A, Syst., Humans*, vol. 28, no. 6, pp. 791–802, Nov. 1998.

Liang Li (S'11–M'13) received the B.S. degree from Xi'an Jiaotong University, Xi'an, China, in 2007. He is currently working toward the Ph.D. degree with the Department of Automation, Tsinghua University. Beijing, China.

His research interests include optimal control and estimation theory of switched and hybrid systems.

Wei Dong (S'03–M'07) received the B.S. and Ph.D. degrees from the Department of Automation, Tsinghua University, Beijing, China, in 2000 and 2006, respectively.

He is currently an Assistant Professor with the Department of Automation and the Rail Transit Control Technology Research and Development Center, Tsinghua University. His main research interests include fault diagnosis, modeling, and simulation of complex engineering systems.

Yindong Ji (M'06) received the B.E. and M.S. degrees from Tsinghua University, Beijing, China, in 1985 and 1989, respectively.

He is currently a Professor with the Department of Automation, the Vice President of the Research Institute of Information Technology, and the Director of the Rail Transit Control Technology Research and Development Center, Tsinghua University. His main research interests include digital signal processing, fault diagnosis, and reliability prediction. His current research interests include predictive maintenance and train control systems of high-speed railways.

Zengke Zhang is a professor of Department of Automation, Tsinghua University. His research interests focuses on the motion control and intelligent control.

Lang Tong (S'87–M'91–SM'01–F'05) received the B.E. degree from Tsinghua University, Beijing, China, in 1985 and the M.S. and Ph.D. degrees in electrical engineering from the University of Notre Dame, Notre Dame, IN, USA, in 1987 and 1991, respectively.

In 1991, he was a Postdoctoral Research Affiliate with the Information Systems Laboratory, Stanford University, Stanford, CA, USA. He was the 2001 Cor Wit Visiting Professor with the Delft University of Technology, Delft, Netherlands, and had held visiting positions at Stanford University and the University of California Berkeley, Berkeley, CA, USA. He is currently the Irwin and Joan Jacobs Professor in Engineering with Cornell University, Ithaca, NY, USA. His research interests include statistical signal processing, wireless communications and networking, and information theory.

Dr. Tong has served as an Associate Editor for the IEEE TRANSACTIONS ON SIGNAL PROCESSING, the IEEE TRANSACTIONS ON INFORMATION THEORY, and the IEEE SIGNAL PROCESSING LETTERS. He was named the 2009–2010 Distinguished Lecturer by the IEEE Signal Processing Society. He received the 1993 Outstanding Young Author Award from the IEEE Circuits and Systems Society, the 2004 Best Paper Award (with M. Dong) from the IEEE Signal Processing Society, the 2004 Leonard G. Abraham Prize Paper Award from the IEEE Communications Society (with P. Venkitasubramaniam and S. Adireddy), and the Young Investigator Award from the Office of Naval Research. He was also a corecipient of Seven Student Paper Awards.